

Raman microscopy investigation of beryllium materials

This content has been downloaded from IOPscience. Please scroll down to see the full text.

2016 Phys. Scr. 2016 014027

(<http://iopscience.iop.org/1402-4896/2016/T167/014027>)

View [the table of contents for this issue](#), or go to the [journal homepage](#) for more

Download details:

IP Address: 134.20.11.89

This content was downloaded on 24/05/2017 at 15:16

Please note that [terms and conditions apply](#).

You may also be interested in:

[Hydrogen retention in beryllium: concentration effect and nanocrystalline growth](#)

C Pardanaud, M I Rusu, C Martin et al.

[An overview of the comprehensive first mirror test in JET with ITER-like wall](#)

D Ivanova, M Rubel, A Widdowson et al.

[Growth and characterization of GaN thin film on Si substrate by thermionic vacuum arc \(TVA\)](#)

Mutlu Kundakç, Asim Mantarc and Erman Erdoan

[Laser cleaning of diagnostic mirrors from tungsten–oxygen tokamak-like contaminants](#)

A. Maffini, A. Uccello, D. Dellasega et al.

[Formation of thin tungsten oxide layers: characterization and exposure to deuterium](#)

Y Addab, C Martin, C Pardanaud et al.

[Towards plasma cleaning of ITER first mirrors](#)

L. Moser, L. Marot, B. Eren et al.

[Effects of plasma treatment on surface properties of ultrathin layered MoS₂](#)

Suhhyun Kim, Min Sup Choi, Deshun Qu et al.

[Synthesis and characterization of -MoO₃ microspheres packed with nanoflakes](#)

Rabindar K Sharma and G B Reddy

[Plasma cleaning of beryllium coated mirrors](#)

L Moser, L Marot, R Steiner et al.

Raman microscopy investigation of beryllium materials

C Pardanaud¹, M I Rusu^{1,2}, G Giacometti¹, C Martin¹, Y Addab¹, P Roubin¹,
C P Lungu³, C Porosnicu³, I Jepu³, P Dinca³, M Lungu³, O G Pompilian³,
R Mateus⁴, E Alves⁴, M Rubel⁵ and JET contributors^{6,7}

¹ Aix Marseille Université, CNRS, PIIM UMR 7345, F-13397, Marseille, France

² National Institute of R&D for Optoelectronics INOE 2000, 409 Atomistilor Street, PO Box MG-5, 077125, Magurele, Ilfov, Romania

³ National Institute for Laser, Plasma and Radiation Physics, 077125, Magurele-Bucharest, Romania

⁴ Instituto de Plasmas e Fusão Nuclear, Instituto Superior Técnico, Universidade de Lisboa, Av. Rovisco Pais, 1049-001, Lisboa, Portugal

⁵ Department of Fusion Plasma Physics, Royal Institute of Technology (KTH), SE-100 44 Stockholm, Sweden

⁶ EUROfusion Consortium, JET, Culham Science Centre, Abingdon, OX14 3DB, UK

E-mail: cedric.pardanaud@univ-amu.fr

Received 21 May 2015, revised 13 October 2015

Accepted for publication 6 November 2015

Published 12 January 2016



CrossMark

Abstract

We report for the first time on the ability of Raman microscopy to give information on the structure and composition of Be related samples mimicking plasma facing materials that will be found in ITER. For that purpose, we investigate two types of material. First: Be, W, Be₁W₉, and Be₅W₅ deposits containing a few percents of D or N, and second: a Mo mirror exposed to plasma in the main JET chamber (in the framework of the first mirror test in JET with ITER-like wall). We performed atomic quantifications using ion beam analysis for the first samples. We also did atomic force microscopy. We found defect induced Raman bands in Be, Be₁W₉, and Be₅W₅ deposits. Molybdenum oxide has been identified showing an enhancement due to a resonance effect in the UV domain.

Keywords: Raman microscopy, beryllium containing material, plasma wall interaction

(Some figures may appear in colour only in the online journal)

1. Introduction

In a tokamak, understanding and being able to predict the evolution of the plasma facing components (PFC) that interact with the plasma is one of the keystones to make nuclear fusion a way of producing energy in the future [1]. The PFCs of the future international reactor ITER that will receive most of the particle flux and/or heat loads will be composed of tungsten and beryllium [2]. Mirrors used for optical spectroscopy and imaging systems for plasma diagnostics, less exposed but still interacting with the plasma and impurities, will be made of metals, and first tests have been done

recently in JET with the ITER-like wall (JET-ILW) configuration [3] using molybdenum or rhodium. In that framework, the surface morphology and composition changes under operation that will lead to changes in the material properties have to be measured and understood. The migration and/or melting of elements in the machine [4–6], the production of dust [7], the hydrogen isotope retention with a safety issue [8], the impurity contamination (oxidation,...) [9] and the complex surface erosion [10, 11] have to be taken into account when trying to predict degradation or lifetime of these PFC. Surface characterization tools are then necessary to help with the interpretation.

Among surface characterization tools, Raman microscopy is a nondestructive, non contact, and local ($\approx 1 \mu\text{m}^2$ lateral resolution) technique, and is of interest for the analysis

⁷ See the appendix of F Romanelli *et al* Proceedings of the 25th IAEA Fusion Energy Conference 2014, Saint Petersburg, Russia.

of samples in relation with plasma wall interactions occurring in tokamaks [12]. It is based on the inelastic scattering of visible or UV photons with a lattice quantum vibration (phonon). As the incident photon loses energy corresponding to the quantum vibration of a given chemical bond, this technique gives an information on the chemical composition of the surface probed. It is sensitive to the surrounding of these chemical bonds. It can give information on the structure at the nanometric scale and on defects.

In this paper we study the ability of Raman microscopy to give information on the structure and composition of Be related samples, using first: Be, W, Be_xW_y deposits, without or with D or N and second the JET-92 polycrystalline Mo mirror exposed in JET-ILW during the first mirror test in JET [3]. The paper is organized as follows: experimental details are given in section 2, results corresponding to the two kind of samples are given in sections 3.1, and 3.2, respectively. Conclusions are given in section 4.

2. Experimental details

Depositions of 400 nm thick Be, W and Be_xW_y ($x = 1, y = 9$ and $x = 5, y = 5$ at%) layers were performed on silicon substrates using the thermionic vacuum (TVA) method for which the emission of an electron beam produced by a heated filament is focused using a special Wehnelt device toward an anode connected to a high voltage regulated power supply. More details can be found in [13] and references therein. The TVA plasma spatial localization allows gas injection close to the substrate during the deposition. Partial pressure of the Be/W in the substrate vicinity was in the range 10^{-3} – 10^{-2} Pa. N_2 or D_2 were also introduced to trap N or D. Their partial pressure were two orders of magnitude higher than the one of the metals. Rutherford backscattering measurements (RBS) were carried out with 1.0, 1.4 and 2.0 MeV H^+ and 2.2 MeV He^+ beams for elemental depth profiling and film thickness evaluation. A beam of 2.3 MeV $^3\text{He}^+$ were used for D quantification by nuclear reaction analysis.

We also studied the JET-92 Mo mirror introduced in the JET tokamak in the framework of the First Mirror Test in JET. This mirror was situated only 1.5 cm away from the JET-93 sample studied in [3]. More details on the exact location of these mirrors can be found in this reference. The surface concentrations of Be, C and O (given in 10^{15} atom cm^{-2}) are 3.3–12.5, 34–76, 37, respectively.

Raman spectra were recorded using a Horiba–Jobin–Yvon HR LabRAM apparatus in the backscattering geometry (with x100 objective, with a numerical aperture of 0.9 for $\lambda_L = 514.5$ and 632.8 nm, and x40 for $\lambda_L = 325$ nm). The laser power was kept at ~ 1 mW μm^{-2} . The Raman mapping mode was also used, and sometimes necessary to increase the signal to noise ratio. Note that to conserve momentum during the scattering (which is a consequence of the system ‘phonon + photon’ being isolated), UV-visible photons can only probe the optical phonons in the center of the Brillouin zone corresponding to the probed crystal. In other words, the equality of the photon momentum (close to $1/\lambda_L$) and the

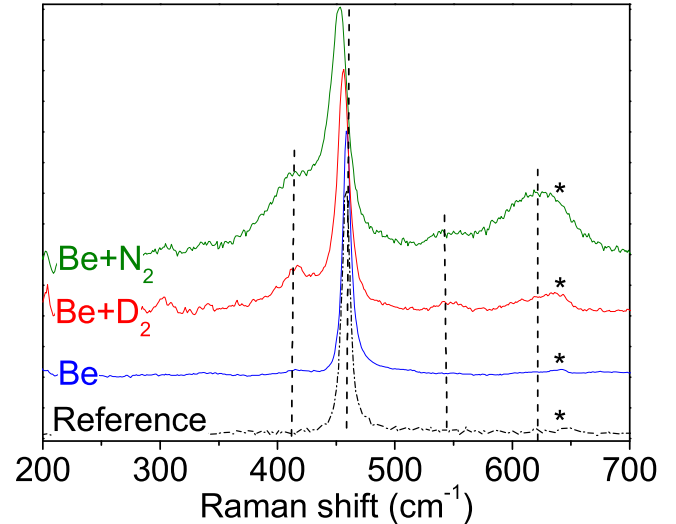


Figure 1. Normalized Raman spectra of Be, Be + D_2 and Be + N_2 samples. The dotted spectrum is Be polycrystalline sample. The star is one of the BeO bands according to [13]. $\lambda_L = 633$ nm.

phonon momentum (ranging from 0 to a value close to $1/a_0$, a_0 being a characteristic crystallographic distance between atoms) can be done only close to zero, which is called the center of the Brillouin zone. It is called the $q = 0$ selection rule in the literature. The AFM (an AFM-NTMDT solver) was used in the tapping mode.

3. Results and discussions

3.1. Be, W and Be_xW_y deposits

Figure 1 displays the Raman spectra ($\lambda_L = 633$ nm) of Be deposited by the TVA method, in presence of N_2 , D_2 or without injected gas. The three spectra are compared to that of a commercial polycrystalline sample. The Be deposited sample is similar to that recorded on the reference crystalline sample taken as a reference, with a small full width at half maximum (8 cm^{-1}): this means that the Be deposited sample is crystalline. The position of the Be stretching band is 459 cm^{-1} . Compared to this spectrum, the sample deposited with D_2 shows a 3 cm^{-1} downshift, a FWHM increase (11.5 cm^{-1}) and three new bands appear at 413, 548 and 634 cm^{-1} , the last one being close to the 645 cm^{-1} band attributed to beryllium oxide [14] (marked by a star in figure 1). The sample deposited with N_2 shows a 6 cm^{-1} downshift of the Be stretching band, a FWHM increase (17 cm^{-1}). They are defect induced bands due either indirectly to Be–D or Be–N bonds or directly to defects caused during the bombardment.

These observations can be related to AFM observations (not shown here) showing the existence of a nanometric roughness which may be related to the existence of underlying nanometric crystallites. When the size of crystallites is about few nanometers, as the phonon in the nanometric crystallite is very well localized and due to the Heisenberg principle, its momentum is not well defined. This phonon

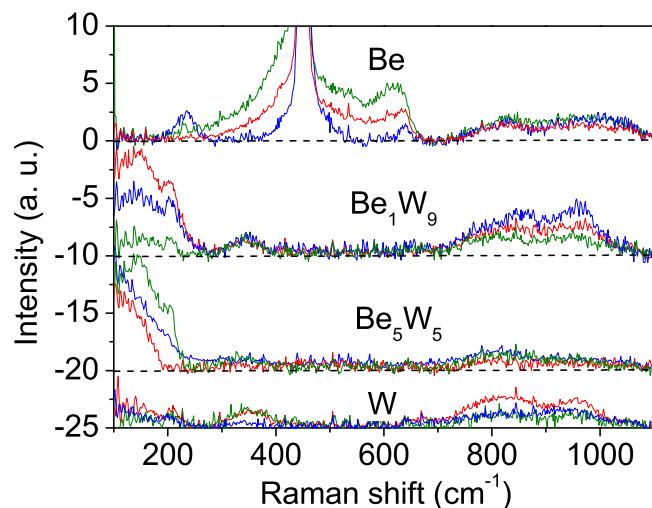


Figure 2. Raman spectra of the pristine Be, W, Be_1W_9 and Be_5W_5 samples deposited by TVA method. Color legends are the same as in figure 1. $\lambda_L = 514$ nm.

confinement (see the related paragraph of [15] and references therein) can then lead to the presence of new frequencies/bands in the spectra and/or change the shape of a given band, which could explain the defect induced band we reported. We will study in more details this point in another publication.

Figure 2 displays the Raman spectra of Be, W, Be_1W_9 and Be_5W_5 deposited without or with D_2 or N_2 . For the Be sample (top spectra), the bands in the $700\text{--}1100\text{ cm}^{-1}$ region are attributed to beryllium oxide. For W deposited (bottom spectra) without or with D_2 or N_2 , the Raman spectra should be flat, according to the $q = 0$ selection rule. The weak bands observed at 350 cm^{-1} and in the $700\text{--}1000\text{ cm}^{-1}$ region that we attribute to surface tungsten oxide are due to air contamination when storing the sample at ambient conditions. For Be_1W_9 (middle spectra) without and with D_2 or N_2 , as for Be_5W_5 , no more Be stretching band is observed at 459 cm^{-1} , meaning Be is bonded with W to form an alloy. Surface tungsten oxide is visible, with a diminution noticed for the Be_5W_5 samples, due to a lower amount of W under the laser beam compared to Be_1W_9 or W samples. Two new bands appear at 139 and 206 cm^{-1} . Their shape is roughly the same whatever the sample, meaning it is not attributed to a bond involving deuterium nor nitrogen. The Be/W atomic ratio are 0.097 , 0.125 and 0.110 for Be_1W_9 without and with D_2 or N_2 , respectively. It is 1.45 , 0.90 and 1.02 for Be_5W_5 without or with D_2 or N_2 , respectively. The intensity of these 139 and 206 cm^{-1} bands is hard to interpret as we noticed it can vary from one location of a sample to another location. Note that the amount of N ($3\text{--}8\text{ at}\%$) or D ($<0.4\text{ at}\%$) does not influence so much the spectra for W and Be_xW_y samples. The 139 and 206 cm^{-1} bands are then not related to the amount of D or N but may be attributed to a selection rule relaxation due to a folding of the W acoustic phonon dispersion putting at the center of the Brillouin zone all the vibrations because of Be impurities. The phonon density of state of W is double and close in frequency to the bands found, which supports the attribution [16].

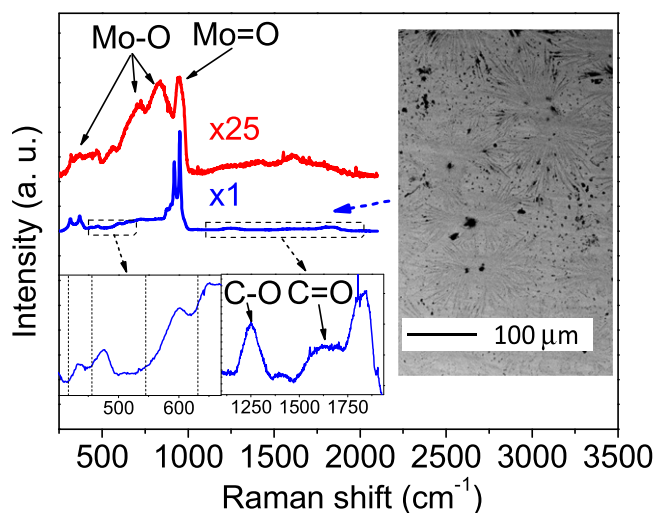


Figure 3. JET-92 mean Raman spectra corresponding to two zones on the sample. The upper spectrum is representative of the majority of the sample. The lower one is representative of a $\approx 0.5 \times 0.5\text{ mm}^2$ region (right inset). $\lambda_L = 325$ nm.

The oxygen content is 9 and $3.3\text{ at}\%$ in $\text{Be} + \text{D}_2$ and $\text{Be} + \text{N}_2$ samples, respectively. For the Be film the results did not give a conclusive evidence for the presence of oxygen above the detection limit, $0.1\text{ at}\%$ in the spot analyzed. The results do not contradict the Raman since the presence of an inhomogeneous distribution of BeO diluted in the film would be difficult to be determined by RBS. The oxygen content in the W, $\text{W} + \text{D}_2$ and $\text{W} + \text{N}_2$ could not be measured by RBS analyses.

3.2. Be containing deposit in Mo JET mirror

Raman spectra with $\lambda_L = 514$ nm were first obtained on the JET-92 sample, with a very poor signal to noise ratio, not exploitable. Using $\lambda_L = 325$ nm improved drastically the situation, meaning the laser used is in resonance with an electronic level of the solid [17]. Figure 3 displays two Raman spectra obtained by summing spectra recorded on two $\approx 25 \times 25\text{ }\mu\text{m}^2$ zones (i.e. Raman mappings mode), using $\lambda_L = 325$ nm. The zones of interest are at the center of the sample (representative of the majority of the sample surface), and at one corner. On most of the surface, optical microscopy show the existence of homogeneously distributed micrometric dots, but on the corner zone, some micrometric radial patterns have been observed by electron and atomic force microscopies (see figure 3 inset for electron microscopy), with ≈ 10 nm height (AFM measurements not shown here). The origin of such patterns is unknown. Everywhere except on such patterns, spectra are mainly due to molybdenum oxide, as in [18]. Bands at ≈ 500 , 700 , and 830 cm^{-1} are attributed to bulk Mo-O bonds, and one band at 950 cm^{-1} is attributed to surface Mo=O bonds. On the pattern, the signature is several times higher (≈ 25 times) than everywhere on the sample, and the spectrum is changed, being composed mainly of two very thin and intense bands at 919 and 951 cm^{-1} . A band observed at 1830 cm^{-1}

may be due to a combination of the two last bands, exhibiting anharmonic effects [19]. Bands attributed to C–O and C=O bands are observed at 1250 and 1640 cm^{-1} . In the 400–700 cm^{-1} , several bands are observed close to the position of the defect induced bands in beryllium, shown in figure 1, but with no clear origin. The doublet at 919/951 cm^{-1} is related to Mo=O bonds. One possible interpretation is that the two frequencies are attributed to two surface Mo=O environments. As the top layer (few nm) contains C and Be, it could reasonably be interpreted as due to Be or C bonded on the surface oxygen atoms.

The origin of this oxide formation is not yet clear but may partially be due to air storage of the Mo mirrors before they were transferred in JET, as mentioned in [3]. The same analysis realized on Mo mirrors stored in air for some years and not exposed in JET should be done to answer the question of the role of oxygen impurities on JET mirrors.

4. Conclusion

We demonstrate the ability of Raman microscopy to give information on the way elements are bonded on PFC containing Be. The presence of defect bands in the deposited Be (400–640 cm^{-1} spectral window) and deposited Be_xW_y (139 and 206 cm^{-1} bands) were observed in the samples. We also report on the detection of Molybdenum oxide formed on the Mo mirror after submitted to plasma wall interactions in JET-ILW. We also report on the existence of a UV Raman resonance effect that increases significantly the Raman signal, allowing to show bulk Mo–O bonds, surface Mo=O bands, and possibly bond creation between surface oxygen and Be or C. This UV resonance coincides with the reflectivity degradation reported in the 250–400 nm range. Mo=O bonds are exalted 25 times on some nanometric roughness found on a $0.5 \times 0.5 \text{ mm}^2$ zone. The results put in evidence the potential of Raman microscopy to study qualitatively PFM evolution due to operations but a more systematic comparison with controlled laboratory samples made in controlled conditions is necessary.

Acknowledgments

This work has been carried out within the framework of the EUROfusion Consortium and has received funding from the Euratom research and training program 2014–2018 under grant agreement No 633053. The views and opinions expressed herein do not necessarily reflect those of the European Commission. C Pardanaud and MI Rusu acknowledge the *Fondation Aix-Marseille Université* for funding the postdoctoral position. This work has also been carried out thanks to the support of the A*MIDEX project (no ANR-11-IDEX-0001-02) funded by the ‘Investissements d’Avenir’ French Government program, managed by the French National Research Agency (ANR).

References

- [1] Neu R *et al* 2011 *Plasma Phys. Control. Fusion* **53** 124040
- [2] Philipps V 2011 *J. Nucl. Mater.* **415** S2–9
- [3] Ivanova D *et al* 2014 *Phys. Scr.* **T 159** 014011
- [4] Coenen J W *et al* 2013 *Nucl. Fusion* **53** 073043
- [5] Krieger K *et al* 2013 *J. Nucl. Mater.* **438** S262–6
- [6] Schmid K, Reinelt M and Krieger K 2011 *J. Nucl. Mater.* **415** S284–8
- [7] Rosanvallon S, Grisolia C, Delaporte P, Worms J, Onofri F, Hong S H, Counsell G and Winter J 2009 *J. Nucl. Mater.* **386–88** 882–3
- [8] Loarer T *et al* 2007 *Nucl. Fusion* **47** 1112–20
- [9] Tsitrone E 2007 *J. Nucl. Mater.* **363–65** 12–23
- [10] Mellet N *et al* 2014 *Nucl. Fusion* **54** 123006
- [11] Brezinsek S *et al* 2014 *Nucl. Fusion* **54** 103001
- [12] Pardanaud C, Addab Y, Martin C, Roubin P, Pegourié B, Oberkofler M, Köppen M, Dittmar T and Linsmeier C 2015 *Phys. Status Solidi c* **12** 98–101
- [13] Lungu C P *et al* 2014 *Vacuum* **110** 207–12
- [14] Jahn M, Mueller M, Endlich M, Neel N, Kroeger J, Chis V and Hellsing B 2012 *Phys. Rev. B* **86** 085453
- [15] Gouadec G and Colomban P 2007 *Progr. Cryst. Growth Charact.* **53** 1
- [16] Crocombette J-P, Notargiacomo P and Marinica M-C 2015 *J. Phys.: Condens. Matter* **27** 165501
- [17] Li C 2003 *J. Catal.* **216** 203–12
- [18] Rouhani M, Hobley J, Subramanian G S, Phang I Y, Foo Y L and Gorelik S 2014 *Sol. Energy Mater. Sol. Cells* **126** 26–35
- [19] Kim H, Kosuda K M, Van Duyne R P and Stair P C 2010 *Chem. Soc. Rev.* **39** 4820–44